Magnetic study of the $Ce_2Fe_{17}H_x$ compounds: Magnetic circular x-ray dichroism, x-ray-absorption near-edge structure, magnetization, and diffraction results

O. Isnard
Institut Laue-Langevin, Boite Postale 156, 38042 Grenoble Cedex, France

S. Miraglia and D. Fruchart
Laboratoire de Cristallographie du CNRS, associé à l'Université J. Fourier, Boite Postale 166, 38042 Grenoble Cedex 09, France

C. Giorgetti, S. Pizzini, E. Dartyge, and G. Krill
Laboratoire pour l'Utilisation du Rayonnement Electromagnétique, Bâtiment 209D, Université Paris-Sud, 91405 Orsay, France

J. P. Kappler
Institut de Physique et de Chimie des Matériaux de Strasbourg Groupe d'Etude des Matériaux Métalliques, Université Louis Pasteur, 67070 Strasbourg, France
(Received 20 December 1993)

Hydrogen insertion in the $Ce_2Fe_{17}H_x$ system leads to spectacular changes of the physical properties. A relative increase of the Curie temperature of almost 100% is observed as well as the highest volume increase. In addition to previous neutron diffraction measurements which pointed out an increase of the local iron moments, we present in this paper absorption and magnetic circular x-ray dichroism (MCXD) experiments performed at the $L_{2,3}$ edges of Ce and the K edge of iron. These measurements allow us to study the evolution of the Ce electronic structure upon hydrogen insertion. Values for the Ce valence have been derived from both absorption and MCXD signals. The MCXD data are analyzed for their shape, intensity, and sign, and compared to the macroscopic magnetic measurements. It is shown that in these compounds the Ce atoms bear a $5d$ magnetic moment, which is coupled antiferromagnetically to that on iron. There is no orbital contribution to this $5d$ moment which is thus solely of spin origin. The values of the $5d$ moment are deduced as a function of each composition in the $Ce_2Fe_{17}H_x$ system at low and room temperature. At the K edge of iron, the shape and intensity of the dichroic signal have been related to the filling of the majority $3d$ band.

I. INTRODUCTION

R_2Fe_{17} compounds (R = rare-earth metal) are known to crystallize with either the rhombohedral Th_2Zn_{17} structure-type or hexagonal Th_2Ni_{17} structure-type for the lighter and heavier rare-earth metals, respectively. This series gained back interest, since it was shown that insertion of light interstitial atoms, such as H,[1] C,[2,3] or N,[4] could raise the usually low Curie temperature of the ferromagnetic compounds.

Substantial improvements in the magnetic properties have been achieved by alloying with carbon and more recently, nitrides of R_2Fe_{17} prepared by gas-solid reaction of N_2 and finely ground powder samples have been reported. In order to have a better understanding of these spectacular effects a lot of characterizations have been carried out using x-ray, and neutron-diffraction, and magnetization measurements. The $R_2Fe_{17}N_3$ compounds are among the best candidates for permanent magnetic applications.

In this study we focused on the cerium based compounds, which are a matter of interest. Particularly several points need to be clarified.

(i) A relative increase of the Curie temperature of almost 100% occurs upon hydrogenation, whereas a relative increase of 50% is usually observed for the other rare earths. Besides, the highest relative volume increase (for a normalized hydrogen uptake) is also observed in the cerium compounds.

(ii) We also have to account for the slight, however significant, increase of the iron moment, which is induced by hydrogenation and that has been observed by neutron diffraction measurements.

In this respect, absorption and magnetic circular x-ray dichroism (MCXD) experiments at the $L_{2,3}$ edges of cerium and K edge of iron are particularly suitable, since they allow us to probe directly the local states of iron and cerium and the valence of the latter species as well.

II. EXPERIMENTAL DETAILS

The alloys were melted in a HF induction furnace from very pure starting elements and then annealed at 850 °C for one week. Standard x-ray-diffraction experiments revealed the samples to be mainly single phase; these rhombohedral compounds were indexed using the hexagonal multiple cell.

Hydrogenation was performed in dedicated autoclaves at a rather moderate pressure of 5 MPa, and at $T=435$ K. The interstitial uptake resulting from these solid-gas

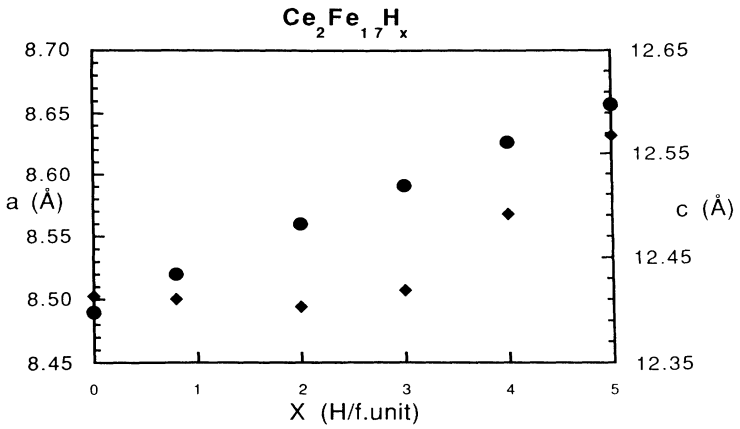

FIG. 1. Evolution of the cell parameters a,c solid dots, and with the amount of hydrogen ($\times$) accommodated in the structure of the $Ce_2Fe_{17}H_x$ compounds.

reactions was determined by volumetric and gravimetric methods. Details on the neutron-diffraction experiments, which allowed us to determine the interstitial location and to refine the magnetic structures have been reported elsewhere.[1]

The Curie temperatures were determined using a Faraday-type torque balance. The magnetic measurements were carried out in the range 4.2–300 K using an axial extraction magnetometer operating at fields up to 6 T.

MCXD spectra were recorded at LURE using a position sensitive detector in transmission mode at 0.3 mrad below the orbit plane (i.e., for about 80% right circularly polarized light). The procedure of data collection and the experimental setup are described elsewhere.[5,6] The switching field used to polarize the samples, while recording the MCXD signal was 1 T at room temperature. For experimental reasons, it was significantly lower for the low-temperature measurements: 0.6 T at the Ce L edges and 0.3 T at the Fe K edge, leading for instance to 80 and 55 % of the saturation magnetization, respectively for $Ce_2Fe_{17}H_5$.

III. STRUCTURAL AND MAGNETIC RESULTS

A. Structural results

X-ray diffraction has shown that the host structure is retained upon interstitial insertion for the cerium series contrarily to what is observed in some 2–17 carbides containing other rare earths. A significant increase of the unit cell volume is observed as well as a fairly anisotropic cell expansion. We have plotted in Fig. 1 the a and c lattice parameters of $Ce_2Fe_{17}H_x$ as a function of x. It is seen that the lattice expansion occurs rather in the basal plane than along the c axis of the hexagonal lattice.

Neutron-diffraction experiments have allowed us to locate the light interstitial elements H (Refs. 1 and 7) and N (Refs. 8 and 9), respectively. Mainly two kinds of available sites have been shown, which are 6-coordinated and 4-coordinated sites, respectively. The 6-coordinated sites can be regarded as distorted octahedra with four iron atoms and two rare-earth atoms at the corners (Fig. 2). Those are the major sites for hydrogen accommodation. A full occupancy of these sites corresponds to the formula $R_2Fe_{17}H_3$. The additional hydrogen atoms ($x=4-5$) are accommodated in tetrahedral sites with two iron atoms and two rare-earth atoms at the corners.[7,10] We performed time-resolved neutron-diffraction experiments in which the "in-beam" desorption of the hydride was studied.[10] These additional measurements, where the hydrogen site occupancy was sequentially followed, have shown that the most stable sites are the octahedral ones. We can thus conclude that they correspond to the stronger binding energy (Fig. 3).

Another important structural feature concerns the increase of some distances induced by interstitial insertion. It must be recalled that in this structure type the ordered

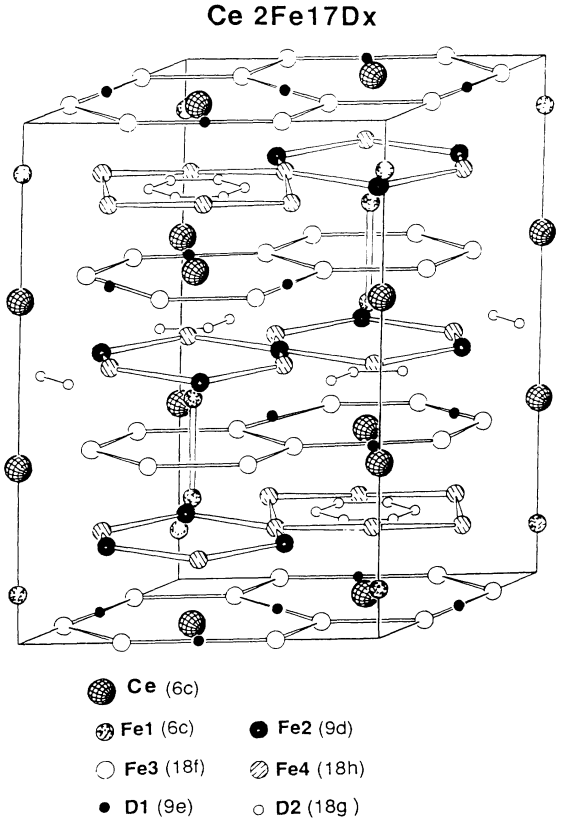

FIG. 2. Crystal structure of the $Ce_2Fe_{17}H_x$ compounds (R-3m space group).

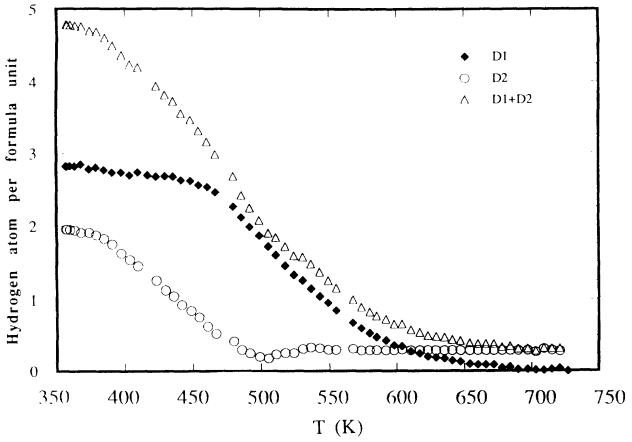

FIG. 3. Deuterium content per interstitial site as a function of temperature (in hydrogen per formula unit) after Ref. 10. The notation of the site is that of Fig. 2.

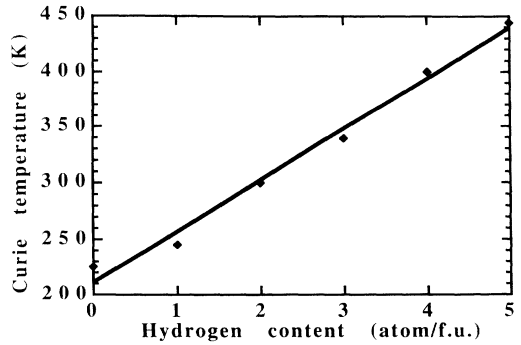

FIG. 4. Plot of the Curie temperature as vs hydrogen content for the $Ce_2Fe_{17}H_x$ series.

substitution of some rare-earth atoms by iron pairs yields Fe-Fe distances as short as 2.33 Å. Neutron-diffraction analysis shows that interstitial insertion gives way to a relaxation of the local stressed parts of the structure.

The cerium coordination in these compounds is rather complicated, since 19 atoms take part in the cerium coordination polyhedron in the host metal. Interstitial insertion gives rise to a 22-coordinated site in the case of $Ce_2Fe_{17}N_3$ and $Ce_2Fe_{17}H_3$, this latter coordination number going up to 24 in the case of $Ce_2Fe_{17}H_5$. Considering these coordination changes, subtle effects on the valence of cerium may be expected. Knowing whether it occurs at a definite interstitial concentration or whether it is an ongoing process that involves an increasing fraction of transformed cerium atoms upon insertion is an open question that prompted the MCXD experiments the results of which are reported below.

B. Magnetic results

We have reported in Table I some relevant magnetic data. It is seen that interstitial insertion drastically affects the bulk magnetic properties. Ce_2Fe_{17} exhibits a helimagnetic structure below the Néel temperature $T_N=225$ K, whereas the fully charged hydride $Ce_2Fe_{17}H_5$ exhibits a ferromagnetic transition at $T_c=444$ K.[11] Figure 4 illustrates the transition temperatures as a function of the hydrogen content in the $Ce_2Fe_{17}H_x$ system.

Regarding the magnetization behavior, a spectacular modification of the saturation process is observed upon hydrogenation (Fig. 5). The helimagnetic structure of the starting alloy is ascribed to result from a balance between negative and positive Fe-Fe exchange interactions. It is felt that interstitial insertion allows the relaxation of some parts of the lattice thus favoring the positive interactions and destabilizing accordingly the helimagnetic structure in order to give place to a ferromagnetic structure.

Neutron-diffraction experiments point out an increase of about 7.5% of the local iron moments upon hydrogenation. Besides, they have allowed us to distinguish the iron sites for their moments, e.g., it is seen that the dumbbell sites bear higher moments than other iron sites do. It is worth mentioning also that they do not reveal (within the experimental resolution) a moment on cerium atoms. It is not possible to conclude whether this is due to a weakness of such a contribution or to the true lack of long-range magnetic order. These results strongly suggest that the site occupancy and the magnetism of iron are the relevant parameters for the hydrogen-induced changes of the physical properties. For example, we have to understand whether the picture of a weak ferromagnetic state transforming towards a strong ferromagnetism state for iron holds in the present case. For this additional purpose we carried out the MCXD experiments, which are hereafter discussed.

IV. SPECTROSCOPIC ANALYSIS OF THE $Ce_2Fe_{17}H_x$ SYSTEM

In order to investigate the effect of hydrogen on the physical properties of the $Ce_2Fe_{17}H_x$ phases, we have

TABLE I. Structural and magnetic parameters of the $Ce_2Fe_{17}H_x$ series.

X (atom/f.u.)	a (Å)	c (Å)	V(Å 3)	Octaedra (atom/f.u.)	Tetraedra (atom/f.u.)	T_c (K)	M_S 4 K (μ_B/f.u.)
0	8.490	12.413	774.8	0	0	225	30.46
1	8.520	12.411	780.2	1	0	245	31.18
2	8.560	12.403	787.1	2	0	300	32.03
3	8.591	12.419	793.7	3	0	339	32.53
4	8.626	112.491	805.1	3	1	400	33.97
5	8.657	12.568	815.7	3	2	444	35.35

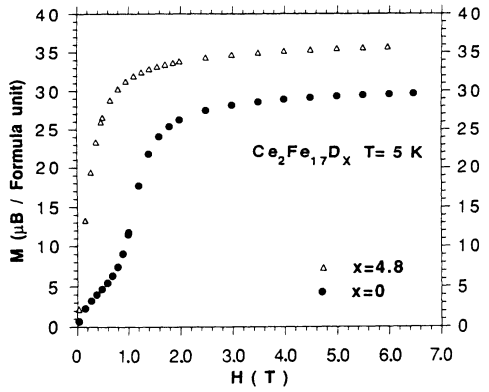

FIG. 5. Magnetization as function of applied field for $Ce_2Fe_{17}H_5$ (open symbol) and Ce_2Fe_{17} (filled circle) at $T=5$ K.

performed x-ray-absorption experiments. In a first part, we will focus our attention on the L_3 edge of the Ce atom to study the fluctuation of the Ce valence upon insertion of hydrogen. Then the magnetic circular x-ray dichroism observed on the $Ce_2Fe_{17}H_x$ series, will be analyzed at both L_2 and L_3 absorption edges of Ce and at the K edge of iron. The data will be discussed in terms of magnetic interaction and compared to the macroscopic magnetic measurements presented above. Finally, the results are compared to those of $CeFe_2$ and $CeFe_2H_4$.

A. Study of the XANES at the Ce-L_3 edge

This section deals with the evolution of the valence of Ce in the $Ce_2Fe_{17}H_x$ series. The determination of the valence has been performed using a deconvolution technique from the mixed valent L_3 spectra. The deconvolution process is based on an arctan function, which describes the transition from the $2p$ to the continuum states and Lorentzian functions that take into account both the $5d$ density of unoccupied states and the finite life time of the $2p$ core hole. The method used to extract the Ce valence based on fitting of the intensity ratio of the two white lines is described in details by Röhler.[12,13] The fractional occupation of the $4f$ configurations has been extracted using a least-squares fitting procedure.[14]

It is really important to check how the change in the magnetic properties observed upon hydrogenation is correlated to the change of the electronic structure of cerium. Especially we have to consider the possibility for the occurrence of a Ceα to Ceγ transition.[11,15]

TABLE II. Ce-valence state fitted from the L_3 edge XANES spectra of the $Ce_2Fe_{17}H_x$ compounds.

X (atom/f.u.)	Ce valence	σ (valence)
0	3.33	±0.005
1	3.318	±0.005
2	3.318	±0.005
3	3.290	±0.003
4	3.280	±0.006
5	3.260	±0.003

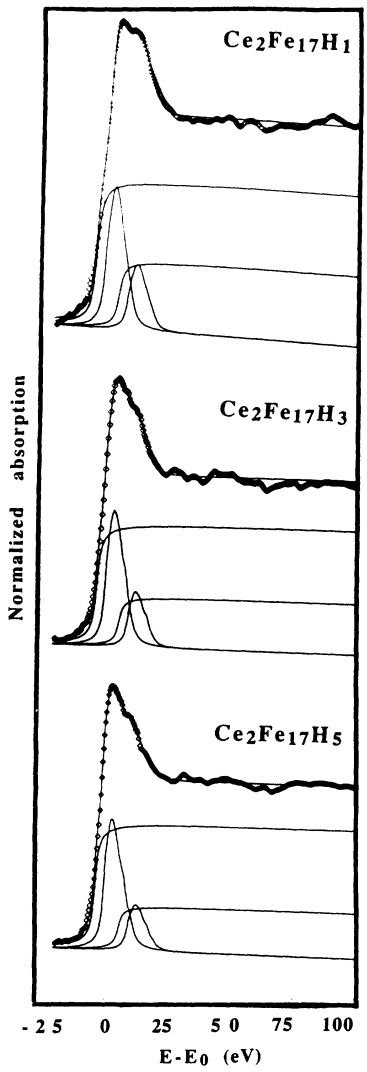

FIG. 6. XANES spectra of some $Ce_2Fe_{17}H_x$ compounds, the solid lines refer to the fitted spectra and the open diamond to the experimental data. The lower curves refer to the arctan and Lorentzian functions of the $4f^1$ and $4f^0$ contributions according to Refs. 12 and 13.

The x-ray absorption near-edge structure (XANES) spectrum of Ce_2Fe_{17} clearly exhibits the two-bump structure associated to $4f^1$ and $4f^0$ channels (Fig. 6). The intensity of the structure associated to the $4f^1$ final states located at lower energy increases with the hydrogen content (x), which indicates a decrease of the Ce valence. However, even in the fully hydrogenated compound $Ce_2Fe_{17}H_5$, both $4f^1$ and $4f^0$ configurations are still present[16] indicating the persistence of a mixed-valent state as seen in Table II. It is thus obvious that in $Ce_2Fe_{17}H_x$ system, unlike in $CeFe_2$, the hydrogenation does not lead to pure trivalent $4f^1$ state as observed in the $CeFe_2H_4$ compound.[5] The evolution of the Ce valence as a function of the cell volume is plotted in Fig. 7. It is important to notice that in the $CeFe_2H_4$ compound, insertion of hydrogen yields to the amorphisation of the $CeFe_2$ crystals (Laves type), whereas in the case of

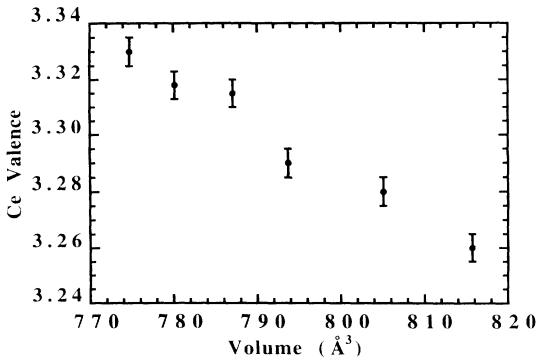

FIG. 7. Evolution of the Ce valence as a function of the cell volume in the $Ce_2Fe_{17}H_x$ series.

the $Ce_2Fe_{17}H_x$ system, the crystal structure of the host alloy is preserved over all the hydrogen composition range. This is probably at the origin for the persistence of a mixed valent state in $Ce_2Fe_{17}H_x$ alloys.

Unlike what is observed for $CeFe_2H_4$, where the hydrogen content is much higher, it is worth noticing a lower change in the $Ce_2Fe_{17}H_x$ system. It seems that the higher H/Ce ratio in $CeFe_2H_4$ and thus a higher hydrogen pressure within the lattice leads to larger effects on the cerium valence than $Ce_2Fe_{17}H_5$.

B. MCXD at L_2 and L_3 edges of Ce

1. Introduction

Linear and circular x-ray photons yield new tools to probe the magnetic polarization at a microscopic scale. Due to the site selectivity and the orbital symmetry selectivity of the core-level spectroscopies. Experimentally, this part of science emerged only a few years ago.[6,18–20] Nevertheless, the phenomena encountered in the magnetic circular x-ray dichroism are getting better understood in the light of recent theoretical work.[21–24] Particularly from MCXD experiment it is shown that orbital and spin contribution to the magnetic moment may be separated.[21]

In this paper we will focus on the MCXD, which is simply the difference of the x-ray-absorption cross section between two experimental situations (the photon helicity being either parallel or antiparallel to the magnetic moments of the samples). In the absence of orbital contribution, it is related to the difference between the spin-up and spin-down density of unoccupied states and thus may be related to the magnetic moments. In the case of the $L_{2,3}$ edges because of the dipolar selection rules, the probed empty states are the $5d$, and the MCXD gives a fingerprint of the $5d$ moment. According to the MCXD studies of $5d$ impurities in iron[20] the interpretation of the dichroic effect is now rather well understood, in the case of $5d$ — transition metal, at the $L_{2,3}$ absorption edges. For instance, MCXD has been successfully used to determine the $5d$ moment as well as the magnetic interactions in several compounds, i.e., Co-Pt.[25] The case of rare-earth $L_{2,3}$ is a little more complex since the MCXD signal may be also sensitive to the localized magnetism of

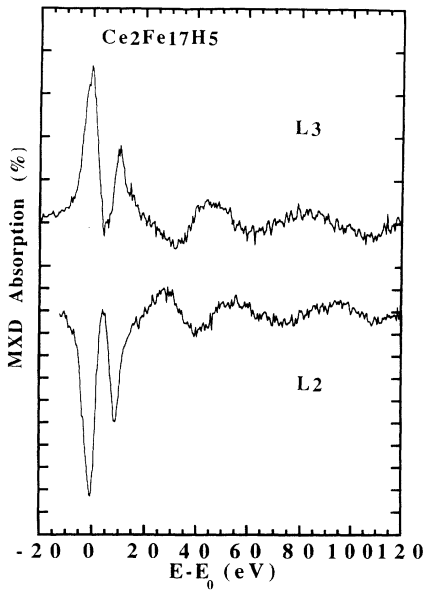

FIG. 8. Example of the branching ratio (-2) followed by the MCXD normalized signal at 300 K for the Ce $L_{2,3}$ edges of $Ce_2Fe_{17}H_5$.

the $4f$ shells via $4f$-$5d$ exchange coupling. We present in this section the results obtained on the $Ce_2Fe_{17}H_x$ alloys ($x=1$, 2, 3, 4, and 5) at both L_2 and L_3 edges.

2. Shape of the MCXD signal of the Ce $L_{2,3}$ edges

As in the $L_{2,3}$ absorption edges of Ce in $Ce_2Fe_{17}H_x$ (Fig. 6) the MCXD signals exhibit a double-peak structure for all the concentrations here studied (Fig. 8). These dichroic features are characteristic of the intermediate valence (IV) state of Ce in intermetallic compound.[17] The double structure is attributed, as for the edge itself, to the two possible screening mechanisms of the $2p$ core hole induced by the strong hybridization between the $4f$ states and the conduction band.[26] This assumption is well confirmed by the fact that the area ratio of the two MCXD peaks is found to be very close to that of the two lines observed on the XANES spectra.

3. Amplitude of the MCXD signal of the Ce $L_{2,3}$ edges

The measurements performed at 20 K for the $Ce_2Fe_{17}H_1$, $Ce_2Fe_{17}H_3$, and $Ce_2Fe_{17}H_5$ at the Ce $L_{2,3}$ edges evidenced that at low temperature the amplitude and shape of the MCXD dichroic effect is the same for all compositions which reflects that these alloys remain in a mixed valent state. Figure 9 shows that the room-temperature MCXD signal is significantly increased by the hydrogen absorption, which simply reflects the increase of the Curie temperature of the $Ce_2Fe_{17}H_x$ alloys on the hydrogen content.

The rather low MCXD signal observed at room temperature for $Ce_2Fe_{17}H_2$ can thus be explained by the vicinity of its Curie point ≈ 300 K. Nevertheless MCXD signals are observed both at L_2 and L_3 edges. When $x=3$ hydrogen atoms per formula unit, the MCXD sig-

nal seems to reach a saturation and it is only slightly higher for the cases where $x > 3$. These observations agree qualitatively well with the shape of a Brillouin function, since for $Ce_2Fe_{17}H_4$ and $Ce_2Fe_{17}H_5$ at room temperature, T_{RT}/T_C is about 0.75 and 0.67, respectively. The dichroic signal should thus be almost at its saturation value, as does the magnetization: M_{RT}/M_S 4.2 K=0.74 and M_{RT}/M_S 4.2 K=0.8, respectively.

Following the conclusion that the $L_{2,3}$ MCXD intensity in IV Ce compounds has the same origin as for 5*d* impurities in iron we may try to deduce the 5*d* magnetic moment from the MCXD experimental spectra of the $Ce_2Fe_{17}H_x$ series. To do so, we have measured the signal area of the $Ce_2Fe_{17}H_x$ MCXD spectra and extracted the 5*d* magnetic moment after scaling with that of $CeFe_2$ and $LuFe_2$. The determinations at room and low temperature are reported in Tables III and IV, respectively. Whereas for all the compositions we found the same 5*d* magnetic moment at low temperature ($\approx 0.4\mu_B$), the values at room temperature are found to increase (up to about $0.5\mu_B$) with the hydrogen content accordingly with T_c. It can be noticed that the intensity of the dichroic effect at 20 K is lower than that observed at 300 K; this is due to the fact that at low temperature, for experimental reasons, the magnetic field used, 0.6 T, is lower than for high temperature 1 T. The as-deduced 5*d* moments are consequently weaker.

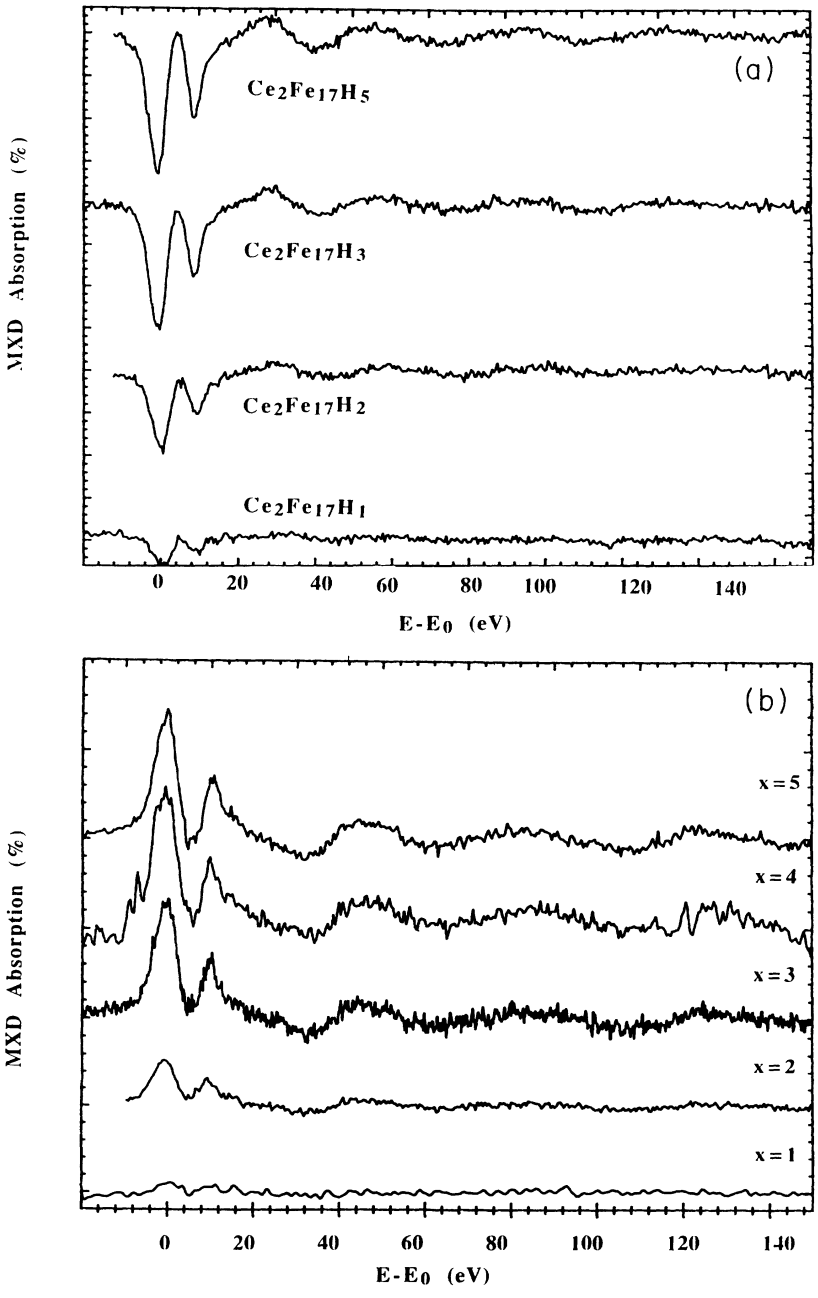

FIG. 9. MCXD normalized spectra at the L_2 (a) and L_3 (b) edges for the $Ce_2Fe_{17}H_x$ series at room temperature. Normalized absorption unit=1%.

TABLE III. Relevant parameters of the dichroic signal recorded at room temperature at the Ce $L_{2,3}$ edges.

Units	$A1$ (%)	$A2$ (%)	$W1$ (eV)	$W2$ (eV)	μ_{exp5d} ($\mu_{B/Ce}$)	ΔE_{MCXD} (eV)	ΔE_{edges} (eV)
$Ce_2Fe_{17}H_1$ L_2	−0.28	−0.15	6.4	4.2	0	9.55	
$Ce_2Fe_{17}H_1$ L_3	0.08				0		8.9
$Ce_2Fe_{17}H_2$ L_2	−1.0	−0.52	5.8	4.8		10	
$Ce_2Fe_{17}H_2$ L_3	0.28	0.16	6.4	4.2	0.22	10.6	8.8
$Ce_2Fe_{17}H_3$ L_2	−1.50	−0.90	5.8	4.2		9.5	
$Ce_2Fe_{17}H_3$ L_3	0.65	0.35	6.4	4.7	0.5	10	8.7
$Ce_2Fe_{17}H_4$ L_3	0.75	0.35	6.4	4.2	0.5	10.6	9.0
$Ce_2Fe_{17}H_5$ L_2	−1.70	−1.0	5.3	4.2		9.5	
$Ce_2Fe_{17}H_5$ L_3	0.75	0.35	5.8	4.2	0.5	10.6	8.9

A careful analysis of the area of the MCXD signal at the L_2 and L_3 edges evidences that the branching ratio (−2) expected by theoretical approaches based on the Erskine-Stern model[27] is observed whatever x in the $Ce_2Fe_{17}H_x$ series (Fig. 9). In the framework of this model, since the branching ratio (−2) is observed for all the $Ce_2Fe_{17}H_x$ compounds, we may safely conclude that no orbital contribution to the Ce $5d$ magnetic moment is present.[21] It has been shown that in presence of pure localized Ce-$4f$ states (as observed in (Ce_3Al_{11} or $CeRu_2Ge_2$), this branching ratio deviates strongly from −2. Such results fully confirm that hydrogenation does not localize the Ce-$4f$ states in the $Ce_2Fe_{17}H_x$ series, unlike that observed in $CeFe_2H_4$.

4. *Sign of the MCXD signal of the Ce $L_{2,3}$ edges*

The MCXD signals obtained at both L_2 and L_3 edges, witness the existence of an ordered $5d$ magnetic moment on the Ce site in these compounds. The multiple scattering theory of MCXD,[28] shows that right circularly polarized light induces preferential transitions towards unoccupied spin-up states (which are aligned in the direction of the photon wave vector, i.e., $+Oz$) at the L_2 edge and spin-down states (i.e., along Oz) at the L_3 edge. Thus, a negative sign of the MCXD signal at the L_2 means that the $5d$ unoccupied state are mainly of spin-down character. As a consequence, the occupied states must be of spin-up character, that is to say the $5d$ magnetic moment is aligned along $-Oz$ when the magnetic field B (M) is applied along Oz.

Since in Ce_2Fe_{17} compounds the Fe contribution to the magnetism is larger than that of the Ce one, the Fe-$3d$ moments are along the Oz axis (along the magnetic field): The spin S_{3d} is along $-Oz$. Furthermore, the interaction between S_{3d} and S_{5d} being always antiferromagnetic, the Ce-$5d$ moment is expected to be along $-Oz$. For the compounds under study, the MCXD signal is negative (positive) at the L_2 (L_3) edges, confirming that the $5d$ magnetic moment is aligned along $-Oz$. Similar results have already been obtained in the $CeCo_5$. $CeFe_2$ and Ce_2Co_{17} system.[5] The schematic representation of the interactions between the magnetic moments deduced from the MCXD experiments for the $Ce_2Fe_{17}H_x$ system, can be given as following:

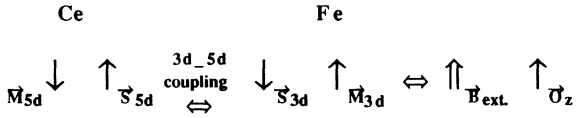

TABLE IV. Relevant parameters of the dichroic signal recorded at low temperature at the Ce $L_{2,3}$ edges. ΔE_{MCXD}: energy splitting of the two contributions in the MCXD signal; ΔE_{edges}: energy splitting of the two lines in $L_{2,3}$ edges; $A1$ ($A2$): amplitudes of the low- (high-) energy (MCXD structures; $W1$ ($W2$): widths at half height of low- (high-) energy MCXD lines; μ_{exp5d}: $5d$ moment extracted from MCXD experiments under 1 T at room temperature and 0.6 T at low temperature.

Units	$A1$ (%)	$A2$ (%)	$W1$ (eV)	$W2$ (eV)	μ_{exp5d} ($\mu_{B/Ce}$)
$Ce_2Fe_{17}H_1$ L_3	0.48	0.33	5.8	3.8	0.37
$Ce_2Fe_{17}H_3$ L_3	0.5	0.34	5.8	4.0	0.4
$Ce_2Fe_{17}H_5$ L_3	0.52	0.35	5.8	4.3	0.4

C. MCXD study at the Fe K edge

1. *Sign of the MCXD signal at the Fe K edge*

The MCXD signal can be described as a two sharp-peak structure of opposite sign. The first peak is ob-

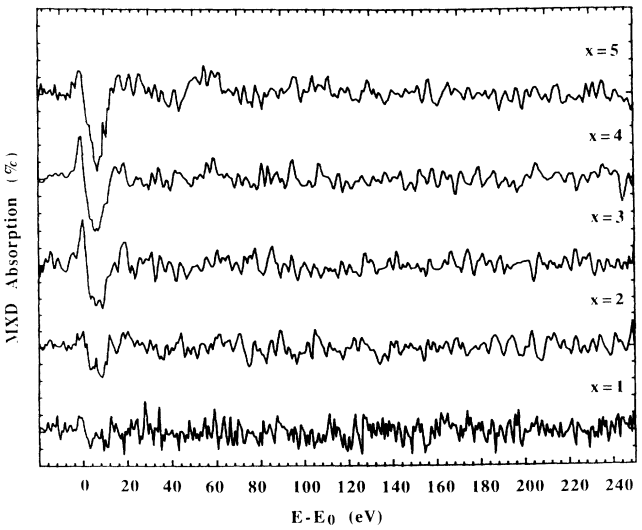

FIG. 10. MCXD normalized spectra of the K edge in the $Ce_2Fe_{17}H_x$ compounds at room temperature. Normalized absorption unit = 1%.

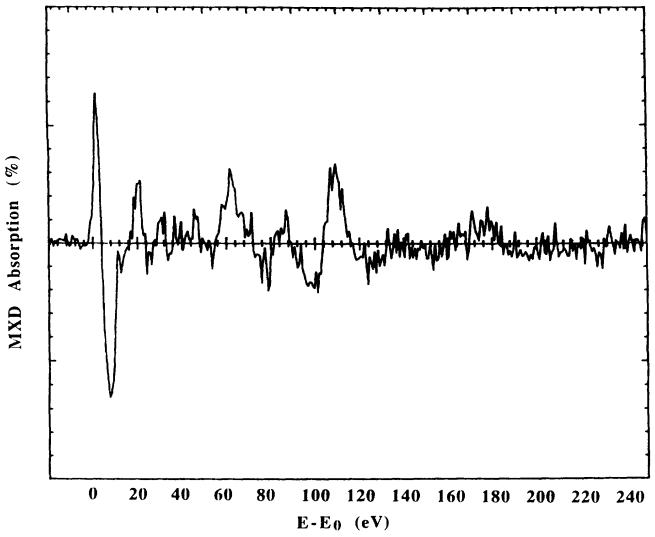

FIG. 11. MCXD normalized spectra of the K edge in the elemental α iron at room temperature. Normalized absorption unit = 1%.

served around E_0 (at the K-edge energy) is found to be positive for both the $Ce_2Fe_{17}H_x$ and the elemental iron (see Figs. 10 and 11). On the other hand, the peak observed at higher energy is negative for the iron as well as for the $Ce_2Fe_{17}H_x$ series. Since the sign of the MCXD signal is related to the direction of the magnetism, it can be deduced that in the $Ce_2Fe_{17}H_x$ compounds the Fe moments are aligned parallel to the external magnetic field (along Oz), confirming the expectation.

2. *Shape of the MCXD signal at the Fe K edge*

Brouder and Hikam[28] have shown that, unlike for R $L_{2,3}$ edges, the relation of the dichroic signal and the magnetic properties is not straightforward. Since there is no spin-orbit in the initial state (K edge) and because spin-orbit coupling interacts directly with the photoelectron, the mechanisms involved in the K edge dichroism are more complex than that of R $L_{2,3}$.

It is to be noticed that the Fe-K edge dichroism observed in these $Ce_2Fe_{17}H_x$ compounds is very similar to that of the elemental iron (Fig. 11).

TABLE V. Fe-K MCXD absolute amplitude $A1$ ($A2$) of the low- (high-) energy peak. Full width at half maximum $W1$ ($W2$) of the low- (high-) energy contribution to the MCXD signal.

Units	($A1$) (%)	$A2$ (%)	$W1$ (eV)	$W2$ (eV)	Area of the second lines (eV)
α-Fe	0.13	−0.13	3	6	−3.4 E-3
$Ce_2Fe_{17}H_1$	0.02		3		−2.1 E-3
$Ce_2Fe_{17}H_2$	0.02	−0.04	3	7.6	−3.7 E-3
$Ce_2Fe_{17}H_3$	0.05	−0.053	3	7.6	−3.7 E-3
$Ce_2Fe_{17}H_4$	0.05	−0.06	3	8	−4.5 E-3
$Ce_2Fe_{17}H_5$	0.03	−0.09	3	7.6	−6.0 E-3

3. *Amplitude of the MCXD signal at the Fe K edge*

It is seen (Fig. 10) that the amplitude of the dichroic signal at the K edge is an order of magnitude smaller than that observed at the L_2 or L_3 edges, leading to smaller signal to noise ratio. The MCXD signal is observed in about 28–30 eV around the K-edge energy in the $Ce_2Fe_{17}H_x$ compounds, whereas in the pure iron the signal is significantly sharper. Since the photoelectron goes to the $4p$ final states, the dichroic effect should be related to the magnetism on the $4p$ unoccupied states (due to intershell polarization and hybridization) that might be reached from the K-edge dichroism.

It is worth noting that in the pure iron, the amplitude of the MCXD peaks is approximately the same, but the full width at half maximum (FWHM) is twice larger for the higher-energy structure than for the lower one. See Table V. The FWHM is found to be the same (about 3 eV) for the first peak in the $Ce_2Fe_{17}H_x$ compounds. The width of the negative peak is significantly broadened up to about 8 instead of 6 eV as observed in the elemental iron. Furthermore, in the $Ce_2Fe_{17}H_x$ compounds, the amplitude of the first peak is always smaller than that of the higher-energy peak. We have recorded low-temperature MCXD spectra as illustrated on Fig. 12 the amplitude of the signal is the same whatever the hydrogen concentration. At low temperature the magnetic field used (0.3 T) was too low to reach saturation of the studied compounds. We will consequently discuss the room-temperature experiments in which the magnetic field was instead high enough (1 T) to saturate the com-

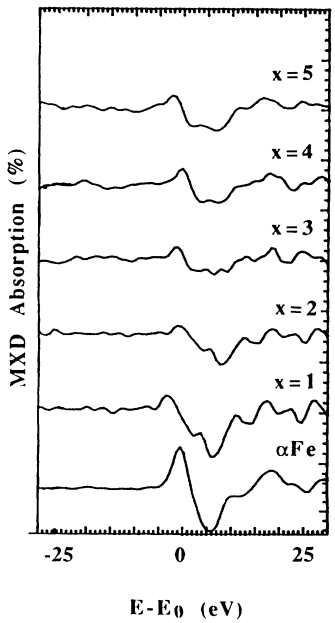

FIG. 12. MCXD normalized spectra of the K edge in the $Ce_2Fe_{17}H_x$ compounds at 4.2 K. Normalized absorption unit = 1%.

pounds. At 300 K, the evolution of the MCXD signal as function of the hydrogen content may be understood in two steps: (i) from $Ce_2Fe_{17}H_1$ up to $Ce_2Fe_{17}H_3$ the dichroism observed at room temperature increases because of the higher-ordering temperature and (ii) from $Ce_2Fe_{17}H_3$ up to $Ce_2Fe_{17}H_5$, the amplitude of the negative peak keeps on increasing, whereas that of the lower-energy peak does not change from 3 to 5 H atoms per formula unit.

It has been suggested recently that the low-energy structure (positive peak) of the K-edge dichroism could give information about the nature of the ferromagnetic state (either weak or strong ferromagnetism) thus giving information on the filling of the $3d$ majority band. This assumption was supported by the fact that whereas elemental iron exhibits a two-peak MCXD effect, only one peak is observed for the well known "strong ferromagnetic metals" as Ni or Co. Pizzini *et al.*[29] have confirmed this experimental trend. By studying Co-Fe multilayers, where a weakening of the first peak (positive one) is observed upon increasing Co concentration and following this interpretation, a decrease of the amplitude of the first MCXD peak in the $Ce_2Fe_{17}H_x$ system could express a progressive filling of the majority $3d$ band,[30] upon hydrogen insertion and then an evolution of the magnetic order from weak ferromagnetic toward stronger ferromagnet. A similar evolution of the MCXD Fe–K-edge spectra has been recently confirmed on other compounds such as $Gd_2Fe_{17}H_5$ or $Nd_2Fe_{17}H_5$, where the shape of the MCXD signal is found to be significantly changed compared to that of pure α-Fe.

V. CONCLUSION

It has been shown that the spectacular change of the physical properties observed upon hydrogenation cannot be related exclusively to a change of the Ce valence. The cell increase is not due to an increase of the Ce radius, since the Ce atoms keep an IV character. The increase of the magnetization induced by hydrogen insertion is neither due to a significant Ce $4f$ contribution to the magnetism, since the mixed valent state ($V=3.3$) has been evidenced both by x-ray spectroscopy and MCXD study. It appears that although the hydrogen insertion is due to the H-Ce interatomic chemical attraction, the effect on the physical properties is rather due to a change of the Fe sublattice. The magnetism on the iron sites is enhanced by H insertion, even if the hydrogen is not attracted by the Fe atoms. The large cell increase may be partly due to an evolution of the Ce valence, nevertheless the main contribution is a relaxation of the stressed (very short) Fe-Fe interatomic distances.

Using the new MCXD technique, we have studied the electronic structure of the $Ce_2Fe_{17}H_x$ series. We have shown that the magnetic moment carried by the Ce atoms in these compounds is essentially of $5d$ character. This Ce-$5d$ moment originates from a strong $3d$-TM (transition metal) polarization. The $L_{2,3}$ edges spectroscopy has shown a delocalized state, which prevents from a localized $4f$ contribution to the magnetism. The MCXD signal is consistent with a complete $4f$ delocalized band and confirms that the itinerant character of the Ce $4f$ states in Ce_2Fe_{17} is retained in these $Ce_2Fe_{17}H_x$ compounds.

[1]O. Isnard, S. Miraglia, J. L. Soubeyroux, D. Fruchart, and A. Stergiou, J. Less-Common. Met. **102**, 273 (1990).

[2]K. H. J. Buschow, T. H. Jacobs, and W. Coene, IEEE Trans. Magn. **MAG-26**, 1364 (1990).

[3]K. H. J. Buschow, R. Coehoorn, D. B. d. Mooij, K. d. Waard, and T. H. Jacobs, J. Magn. Magn. Mater. **92**, L35 (1990).

[4]J. M. D. Coey and H. Sun, J. Magn. Magn. Mater. **87**, L251 (1990).

[5]J. M. Baudelet, E. Dartyge, G. Krill, J. P. Kappler, C. Brouder, M. Piecuch, and A. Fontaine, Phys. Rev. B. **43**, 5857 (1991).

[6]F. Baudelet, C. Brouder, E. Dartyge, A. Fontaine, J. P. Kappler, and G. Krill, Euro. Phys. Lett. **13**, 751 (1990).

[7]O. Isnard, S. Miraglia, J. L. Soubeyroux, and D. Fruchart, Solid State Commun. **81**, 13 (1992).

[8]O. Isnard, S. Miraglia, J. L. Soubeyroux, J. Pannetier, and D. Fruchart, Phys. Rev. B **45**, 2920 (1992).

[9]O. Isnard, S. Miralgia, J. L. Soubeyroux, and D. Fruchart, J. Alloys. Comp. **190**, 129 (1992).

[10]O. Isnard, J. L. Soubeyroux, S. Miraglia, D. Fruchart, L. M. Garcia, and J. Bartolome, in *International Conference on Neutron Scattering* [Physica B **180-181**, 629 (1991)].

[11]O. Isnard, S. Miraglia, D. Fruchart, and J. Desportes, J. Magn. Magn. Mater. **103**, 157 (1991).

[12]J. Röhler, J. Magn. Magn. Mat. **47-48**, 175 (1985).

[13]J. Röhler, in *Handbook on the Physics and Chemistry of Rare Earths,* edited by K. A. Gschneidner, J. R. Eyring, and S. Hufner (North-Holland, Amsterdam, 1987), Vol. 10.

[14]P. Wolfers, in *Conference on Neutron Scattering Data Analysis,* edited by M. W. Johnson (Institute of Physics Conference, England, 1990), pp. 127–134.

[15]D. C. Koskenmaki and K. A. Gschneider, in *Handbook on the Physics and Chemistry of Rare Earths* (Ref. 13).

[16]J. Garcia, J. Bartolome, M. S. D. Rio, A. Marcelli, D. Fruchart, and S. Miraglia, Z. Phys. Chem. Neue. Fol. **163**, 277 (1989).

[17]C. Giorgetti, S. Pizzini, E. Dartyge, A. Fontaine, F. Baudelet, C. Brouder, G. Krill, S. Miraglia, D. Fruchart, and J. P. Kappler, Phys. Rev. B **48**, 12 732 (1993).

[18]G. Schütz, W. Wagner, W. Wilhelm, P. Kienle, R. Zeller, R. Frahm, and G. Materlik, Phys. Rev. Lett. **58**, 737 (1987).

[19]G. Schütz, M. Knulle, R. Wiennke, W. Wilhem, W. Wagner, P. Kienle, and R. Frahm, Z. Phys. B Condens. Matter **73**, 67 (1988).

[20]G. Schutz, R. Wienke, W. Wilhelm, W. Wagner, P. Kienle, R. Zeller, and R. Frahm, Z. Phys. B Condens. Matter. **75**, 495 (1989).

[21]P. Carra, B. T. Thole, M. Altarelli, and X. Wang, Phys. Rev. Lett. **70**, 694 (1993).

[22]B. T. Thole, P. Carra, F. Sette, and G. V. D. Laan, Phys. Rev.

Lett. **68**, 1943 (1992).
[23]M. Altarelli, Phys. Rev. B **47**, 597 (1993).
[24]B. T. Thole and G. V. D. Laan, Phys. Rev. Lett. **67**, 3306 (1991).
[25]S. Ruegg, G. Schütz, P. Fischer, R. Wienke, W. B. Zeper, and H. Ebert, J. Appl. Phys. **69**, 5655 (1991).
[26]J. Hüfner, in *Handbook on the Physics and Chemistry of Rare Earths* (Ref. 13).
[27]J. L. Erskine and A. Stern, Phys. Rev. B **12**, 5016 (1975).
[28]C. Brouder and M. Hikam, Phys. Rev. B **43**, 3809 (1991).
[29]S. Pizzini *et al.* (unpublished).
[30]S. Stähler, G. Schütz, and H. Ebert, Phys. Rev. B **47**, 818 (1993).